HOSTED BY
ELSEVIER
Available online at www.sciencedirect.com
ScienceDirect
Soils and Foundations 61 (2021) 1151–1171
SOILS AND FOUNDATIONS
www.elsevier.com/locate/sandf

Geo-Disaster Report

Reconnaissance report on geotechnical damage caused by 2018 Hokkaido Eastern Iburi earthquake with JMA seismic intensity 7

Tatsuya Ishikawa [a,*], Masayuki Yoshimi [b], Koichi Isobe [a], Shoji Yokohama [a]

[a] *Faculty of Engineering, Hokkaido University, Japan*
[b] *National Institute of Advanced Industrial Science and Technology, Japan*

Received 3 December 2020; received in revised form 21 May 2021; accepted 2 June 2021
Available online 5 July 2021

Abstract

The 2018 Hokkaido Eastern Iburi earthquake with the JMA seismic intensity of 7 occurred at a central south part of Hokkaido, Japan at 3:08 a.m. on September 6, 2018. Considering the social importance of this historical earthquake-induced geo-disaster, the Japanese Geotechnical Society (JGS) organized a "JGS Survey Team for Geotechnical Disasters in Hokkaido, Japan Induced by the 2018 Hokkaido Eastern Iburi earthquake," mainly comprised of experts from the industry and academia of the Hokkaido branch of JGS. The aim of the survey team was to investigate the phenomena and factors which contributed to disaster recovery and disaster prevention/mitigation from both short- and mid- to long-term perspectives, and to provide academic advice to related government organizations. Based on the results of the site investigations conducted by the JGS survey team (JGS, 2019), this report provides a summary of the geotechnical damage caused by 2018 Hokkaido Eastern Iburi earthquake by presenting the detail of strong seismic motion and a various types of geo-disasters which occurred due to the earthquake. Furthermore, this report highlights future research issues on disaster prevention/mitigation in Hokkaido considering the features of the geo-disasters attributed to the earthquake.

Keywords: Geotechnical disaster; Site investigation; Strong seismic motion; Liquefaction (IGC: B4/C0/D7/E8)

1. Introduction

The 2018 Hokkaido Eastern Iburi earthquake, which was a 6.7 magnitude earthquake with a focal depth of approximately 37 km, occurred at a central eastern part of the Iburi area at 3:08 a.m. on September 6, 2018. It is the first time to observe an earthquake with the JMA seismic intensity of 7 in Hokkaido after the seismic intensity of 7 was introduced as the maximum grade by Japan Meteorological Agency (JMA) in 1949. Besides, seismic motion with the JMA seismic intensity of 6 was observed at Mukawa and Hayakita, located within a 25-kilometers epicenter radius. Furthermore, on Ishikari-Yufutsu lowland, approximately 50–80 km far from the epicenter, seismic motions with the JMA seismic intensity of 5–6 were observed. For reference, it is noted that the JMA seismic intensity scale and its estimated physical damages is explained in Fig. 1. The earthquake-induced strong ground motion was observed over the large area of central Hokkaido (Fig. 1). This earthquake caused various types of geo-disasters. Slope failures occurred widely in mountainous areas composed of pyroclastic fall deposit in Atsuma and Abira (Hayakita district) near the epicenter, and liquefaction was observed in some residential areas in Sapporo, 50 km from the epicenter. Fig. 2 shows major investigation sites for geo-disasters by Geological Survey of Hokkaido, with a total number of 419 investigation points. In the figure, the geo-disasters were categorized into two types: one

Peer review under responsibility of The Japanese Geotechnical Society.
* Corresponding author.
E-mail address: t-ishika@eng.hokudai.ac.jp (T. Ishikawa).

https://doi.org/10.1016/j.sandf.2021.06.006
0038-0806/

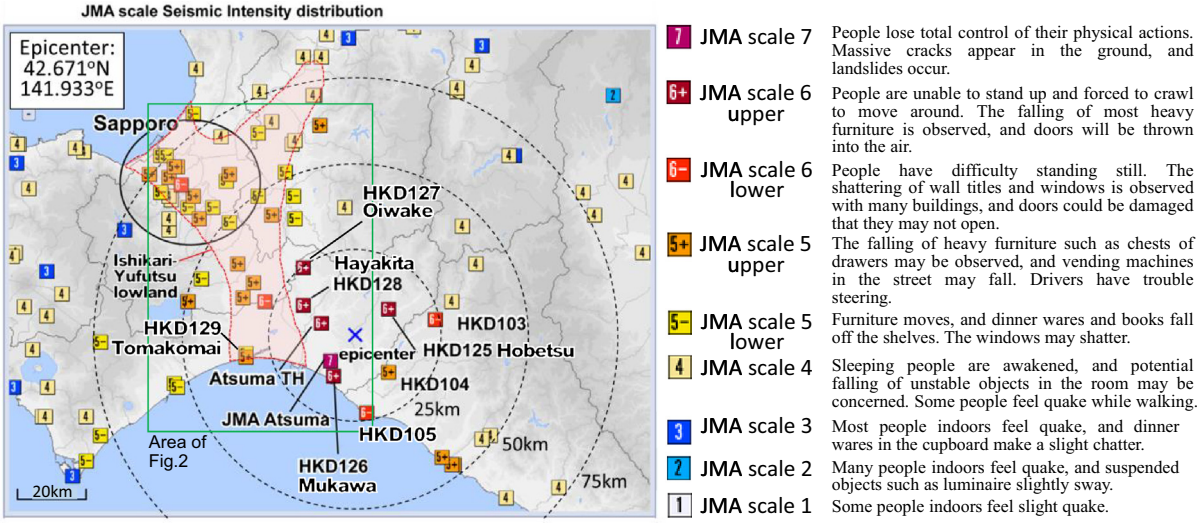

Fig. 1. Seismic intensity distribution of the 2018 Hokkaido Eastern Iburi earthquake (Japan Meteorological Agency, 2019).

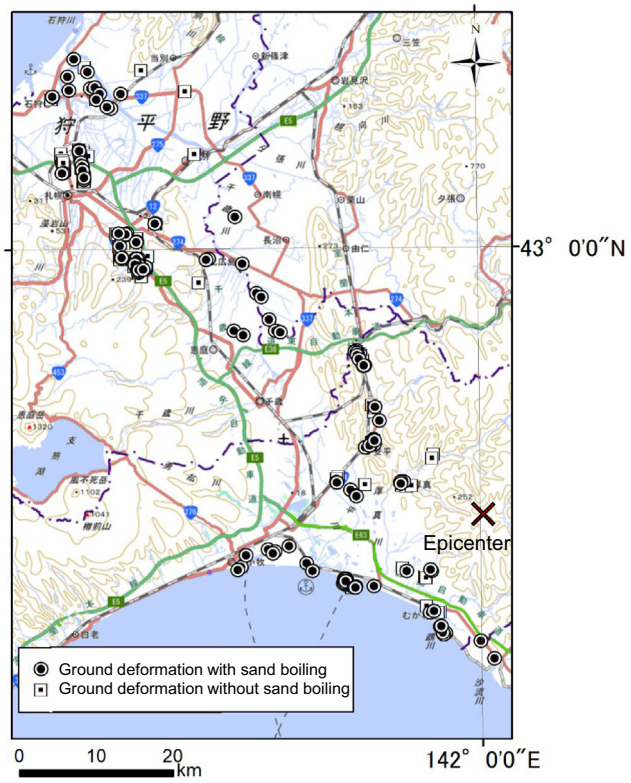

Fig. 2. Investigation sites for geo-disasters by Geological Survey of Hokkaido (created by Hirose, W., HRO).

is geo-disasters due to ground liquefaction with sand boiling, and the other is geo-disasters unrelated to the ground liquefaction, such as slope failure and differential subsidence. A comparison of Fig. 1 with Fig. 2 indicates that the the distribution of the geo-disaster locations corresponds well to the areas with strong seismic motion.

The 2018 Hokkaido Eastern Iburi earthquake resulted in the loss of many lives and seriously affected the daily lives of citizens, as shown in Table 1. According to the public announcement from the Japanese government (Cabinet Office, 2019), 42 people died due to the earthquake, and 462 residential buildings fully collapsed, with 1570 partially collapsed. In the towns close to the epicenter including Atsuma, Abira and Mukawa, many residential buildings were destroyed and many people died in the sediment flows and landslides of volcanic pumice fall deposit induced by strong seismic motion. Some river channels were also blocked by the debris and sediment flows. According to the Ministry of Land, Infrastructure, Transport and Tourism (MLIT, 2018), the estimated total area of slope failures was 13.4 km^2, which was the most severe damage reported for earthquake disasters since the Meiji period (1868–1912). In addition, the earthquake resulted in significant damage in residential areas, farmlands, and to infrastructure (road, port, river, etc), and the lifeline (electricity, water networks) over a wide area in Hokkaido. In particular, many residential buildings in Kiyota-ward, a suburb of Sapporo, unevenly subsided and were tilted by the large-scale ground flow failure induced by the liquefaction of a volcanic soil embankment, with significant damage incurred to these buildings. Also, electric power was lost in Hokkaido following the earthquake partly because of the shutdown of the Tomato-Atsuma Thermal Electric Power Plant in Tomakomai, located near the epicenter. This led to the loss of electricity to 2.95 million households all over Hokkaido for a number of days. This widespread blackout had a serious effect on all of the industries in Hokkaido, including transportation and logistics, agriculture, forestry, and fisheries manufacturing industry, commerce, and tourism.

Kurahashi et al. (2019) reported that, compared with the geo-disaster damage due to previous earthquakes recording the JMA seismic intensity of 7, the 2018 Hokkaido Eastern Iburi earthquake caused an unusually large number of slope failures, as shown in Table 2. In addition, compared

Table 1
Damage caused by the 2018 Hokkaido Eastern Iburi earthquake as of January 28, 2019 (after Cabinet Office, 2019).

Category	Summary of damage
Casualties	Fatalities: 42, seriously injured: 31, slightly injured: 731
Housing damage	Complete collapse: 462, partial collapse: 1570, partial damage: 12,600
Non-residential damage	2456 buildings damaged
Evacuation status	Evacuation notice: 338 peoples of 185 households in 1 city and 4 towns (at maximum) Evacuation recommendation: 2038 peoples of 949 households in 3 towns (at maximum) Number of evacuees: 11,900 (at maximum)
Lifeline damage	Electricity blackouts: about 2.59 million households Water cutoff: up to 68,249 households in 44 cities
Transportation damage	Expressway: 1 line 1 section closed, national highway: no damage, other roads: 16 sections damaged Railway: no damage to facilities, but 6 routes of 4 operators suspended (at maximum) Aviation: no damage to runways, up to 167 flights canceled
River damage	Class A river: 33 locations at 6 rivers in 3 water systems, Class B river: 38 locations at 7 rivers in 6 water systems Dam: 2 river management dams, 3 water supply dams
Sediment disaster	227 locations (Debris flow: 94, landslide: 133)
Damage to harbor facilities	5 ports damaged
Damage to medical facilities	No collapse of medical hospital
Damage to social welfare facilities	171 facilities damaged
Damage to agriculture, forestry and fisheries	Damage amount 114.5 billion yen (accumulation of sediment and damage to farmland and agricultural facilities: 58 billion yen, large-scale collapse of forest land and damage to forest roads: 47.5 billion yen, damage to agricultural products: 8.5 billion yen, damage to fisheries: 510 million yen), Reservoir: no damage
Damage to educational facilities	446 facilities damaged

Table 2
Comparison of the damage with previous earthquakes with seismic intensity 7 (after Kurahashi et al., 2019).

Earthquake name	1995 Kobe earthquake	2004 Niigata Prefecture Chuetsu Earthquake	2011 earthquake off the Pacific coast of Tohoku	2016 Kumamoto earthquake	2018 Hokkaido Eastern Iburi earthquake
Date of occurrence	1995/01/17	2004/10/23	2011/03/11	2016/04/16	2018/09/06
Magnitude	M7.3	M6.8	M9.0	M7.3	M6.7
Focal depth	16 km	13 km	24 km	12 km	37 km
JMA seismic intensity	7 at Kobe, Ashiya, Nishinomiya, and Takarazuka	7 at Kawaguchi	7 at Kurihara	7 at Mashiki	7 at Atsuma
Surface ruptures	Confirmed	Not confirmed	–	Not confirmed	Confirmed
Fatalities and missing	6437	68	22,118	242 (including disaster-related death)	42
Completely collapsed house	104,906	3175	121,768	8672	462
Major disaster factors	House collapse and fire	Landslide	Tsunami	House collapse and slope failure	Slope failure
Number of slope failure points	662 locations	3791 locations	uninvestigated	745 locations	over 6000 locations

to the geo-disaster damage due to other severe earthquakes in Hokkaido, the damage incurred by the 2018 Hokkaido Eastern Iburi earthquake was the most serious ever experienced, as shown in Table 3. According to the Hokkaido government, the total cost of the damage from this earthquake disaster (excluding projects under the direct control of the Japanese government) is 231.99 billion yen (215.70 billion yen due to the earthquake and 16.29 billion yen due to the blackout). Moreover, among the natural disasters that have recently occurred in Hokkaido, the economic loss due to this earthquake surpassed the loss of 1979 billion yen by the August 2016 Hokkaido Heavy Rainfall, and it is the most serious natural disaster in Hokkaido in recent years. Therefore, the Japanese government designated the 2018 Hokkaido Eastern Iburi earthquake a serious disaster in accordance with the law concerning special financial assistance to deal with severe disasters.

Considering the social importance of this historical earthquake-induced geo-disaster, the Japanese Geotechnical Society (JGS) organized a JGS Survey Team for Geotechnical Disasters in Hokkaido, Japan Induced by the 2018 Hokkaido Eastern Iburi earthquake. The team

Table 3
Comparison of the damage with previous earthquakes occurred in Hokkaido (after Hokkaido, 2018a).

Area	Date of occurrence and Earthquake name	Magnitude	Max JMA seismic intensity	Disaster damage
Pacific Ocean side	1952.3.4 1952 Tokachi-oki earthquake	M8.2	5 at Urakawa, Obihiro, and Kushiro	Great damage on the whole Pacific Ocean side. Great tsunami. Fatalities: 28, Missing person: 5, injured: 287. Completely collapsed house: 815, outflow: 91, partially collapsed: 1324.
	1968.5.6 1968 Tokachi-oki earthquake	M7.9	5 at Urakawa, Tomakomai, Hiroo, and Hakodate	Damage mainly in the southwestern region of Hokkaido. Tsunami. Fatalities: 2, injured: 133. Completely collapsed house: 27, partially collapsed: 81.
	1973.6.17 1973 Nemuro-hanto-oki earthquake	M7.4	5 at Kushiro and Nemoro	Damage in Kushiro and Nemuro areas. Tsunami. Injured person: 28. Completely collapsed house: 2, partially collapsed: 1.
	1982.3.21 1982 Urakawa-oki earthquake	M7.1	6 at Urakawa	Damage mainly on the coast of Hidaka area. Small tsunami. Injured person: 167. Completely collapsed house: 13, partially collapsed: 28.
	1993.1.15 1993 Kushiro-oki earthquake	M7.8	6 at Kushiro	Damage mainly in Kushiro and Tokachi areas. Fatalities: 2, injured: 966. Completely collapsed house: 53, partially collapsed: 254.
	1994.10.4 1994 Hokkaido Toho-oki earthquake	M8.1	6 at Kushiro, Akkeshi, and Nakashibetsu	Damage mainly in Nemuro area. Injured person: 436. Completely collapsed house: 61, partially collapsed: 348.
	2003.9.26 2003 Tokachi-oki earthquake	M8.0	6- at Niikappu, Shizunai, Urakawa, Shikaoi, Churui, Makubetsu, Toyokoro, Kushiro, and Akkeshi	Damage in Hidaka, Tokachi, and Kushiro areas. Missing person: 2, injured: 847. Completely collapsed house: 116, partially collapsed: 368.
Japan Sea side	1918.5.26 1918 Rumoi-oki earthquake	M6.0	5 at Onishika and Horonobe	Small damage at Onishika in Rumoi area.
	1940.8.2 1940 Shakotan-hanto-oki earthquake	M7.5	4 at Haboro, Rumoi, Horonobe, Iwanai, and Otobe	Damage mainly in Teshio, Haboro, and Tomamae. Tunami. Fatalities: 10. Completely collapsed house: 26, partially collapsed: 7.
	1983.5.26 1983 Nihonkai-Chubu earthquake	M7.7	4 at Mori and Esashi	Great damage in Toshima and Hiyama areas, especially Okushiri. Great tsunami. Fatalities: 4, injured: 24. Completely collapsed house: 9, partially collapsed: 12.
	1993.7.12 1993 Southwest-off Hokkaido earthquake	M7.8	5 at Otaru, Suttu, Esashi, and Fukaura	Great damage in Toshima and Hiyama areas, especially Okushiri. Great tsunami. Fatalities: 201, missing: 28, injured: 323. Completely collapsed house: 601, partially collapsed: 408.
Inland	1959.1.31 1959 Teshikaga earthquake	M6.3	5 at Kamiosotsubetsu and Akan	Damage mainly in Teshikaga and Akan. Completely collapsed house: 2, partially collapsed: 66.
	1982.1.14 1987 Northern Hidaka Mountains earthquake	M7.0	5 at Kushiro	Damage mainly in Iburi, Tokachi, and Kushiro areas. Injured person: 7.
	2018.9.6 2018 Hokkaido Eastern Iburi earthquake	M6.7	7 at Atsuma	Damage mainly in Iburi and Ishikari areas. Fatalities: 42, injured: 762. Completely collapsed house: 462, partially collapsed: 1570.

was mainly comprising experts from the industry and academia from the Hokkaido branch of JGS. The survey team investigated the phenomena and factors contributing to disaster recovery and disaster prevention/mitigation from short- and mid- to long-term perspectives, and then provided academic advice to related government organizations. Based on the results of the site investigations conducted by the JGS survey team (JGS, 2019), this report provides a summary of the geotechnical damage caused by 2018 Hokkaido Eastern Iburi earthquake with JMA Seismic Intensity 7 by presenting the detail of strong seismic motion and various types of geo-disasters incurred due to the earthquake. Furthermore, this report highlights future research issues on disaster prevention/mitigation in Hokkaido based on the features of the geo-disasters attributed to the 2018 Hokkaido Eastern Iburi earthquake.

1.1. Strong ground motion during 2018 Hokkaido Eastern Iburi earthquake

The source mechanism of the 2018 Hokkaido Eastern Iburi earthquake was a reverse fault with a compression axis in the east-northeast-west-southwest direction. Aftershocks were concentrated in a region approximately 30 km long

extending in the north–south direction with a depth between 15 and 45 km (Fig. 3). The location of the source area is close to the known active fault, but the relation between this earthquake and the active fault is not clear.

Strong ground motion was felt over tcentral Hokkaido during the earthquake. The strong ground motions during the earthquake were well recorded with a nation-wide strong-motion seismograph network, K-NET (Kyoshin Network), and a strong-motion seismograph network KiK-net (Kiban Kyoshi Network) operated by NIED (National Research Institute for Earth Science and Disaster Resilience, 2019), and also with the JMA and Hokkaido prefectural seismograph networks. The observed seismic intensity of the mainshock in the epicentral area was 6− to 6+, third to second highest grades in the JMA scale, and at a seismic station in Atsuma town, it reached 7, the maximum value (Fig. 1). Seismic intensity around Sapporo city was 5- to 6-, the 6th to 8th grade of the 10 grades. Attenuation of the seismic intensity is not uniform with the epicentral distance. Ground motion is considered to be controlled by the subsurface structure of the particular areas (Fig. 4, Yoshida et al., 2007) as well as the distance from the epicentre. The ground motions were strong in the sedimentary basin, Ishikari-Yufutsu basin, in the west of the source area compared with the other mountainous areas.

1.2. Ground motion in the epicentral area

In this section, the characteristics of the ground motions of the mainshock observed in the epicentral area are described. Seismic stations are well located around the epicentral area (Fig. 5). It is noted that the legends for geological maps in Figs. 5 and 10 can be found in the Geological Survey of Japan/AIST (2019). Acceleration waveforms and acceleration response spectra at six seismic stations located at the west of the epicenter (IBUH01, HKD128, Atsuma Townhall, IBUH03, JMA Atsuma, and HKD126) are shown in Figs. 6 and 7. Here, "Sa (h = 0.05)" in Fig. 7 shows the spectral acceleration with a damping ratio (h) of 5%, which is the most common ground motion intensity measure for predicting structural response. The acceleration waveforms of the east–west component are arranged from the northern station to the southern station, and the origin time is set to the time of the earthquake (2018/09/06 03:08:00). The peak ground acceleration of the records shown in Fig. 6 ranges between about 300 – 1000 Gal. The acceleration waveforms observed at south-

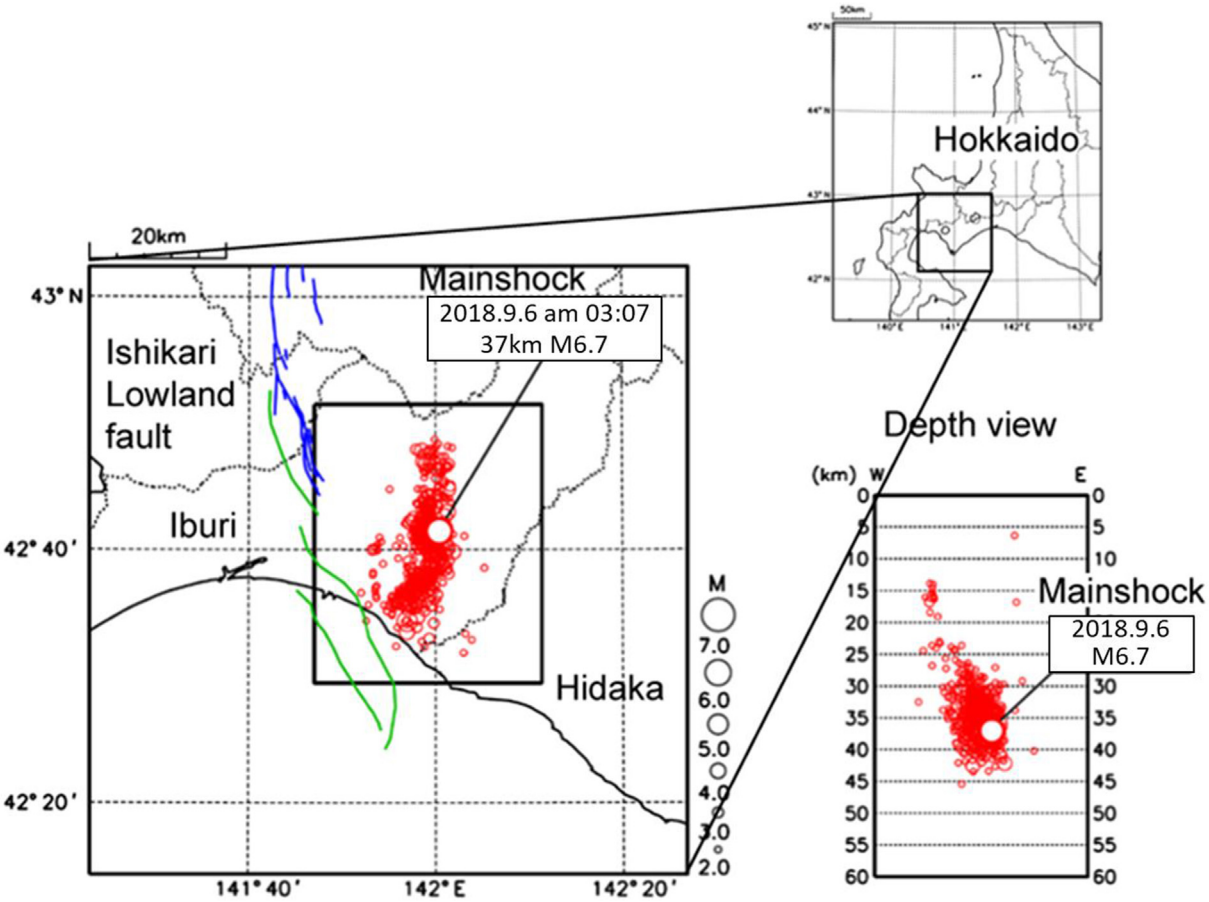

Fig. 3. Mainshock and aftershocks distribution of the 2018 Hokkaido Eastern Iburi Earthquake (Earthquake Research Committee, 2018).

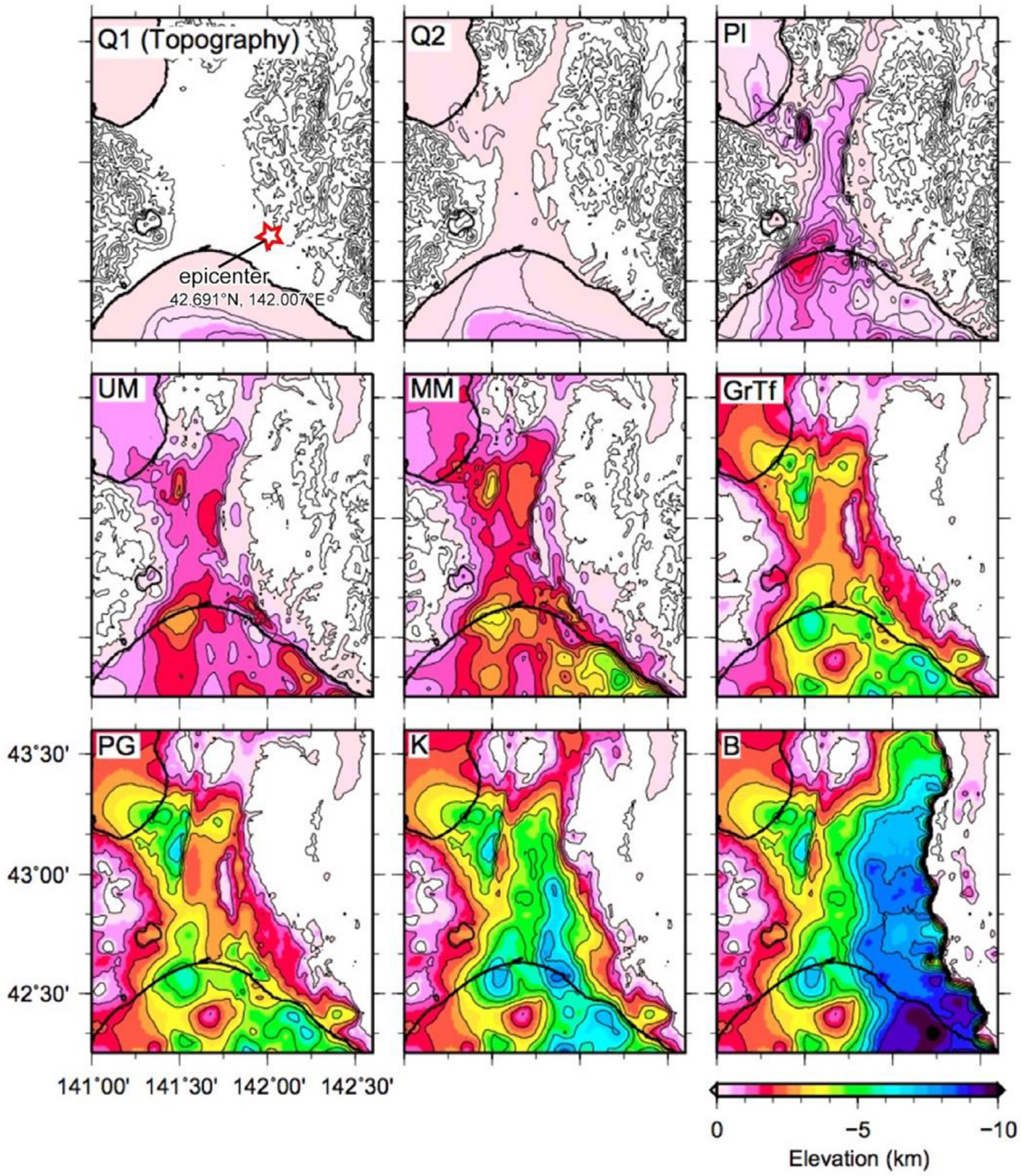

Fig. 4. Velocity structure from the epicenter to the Ishikari lowland (Q2: Lower Pleistocene, Pl: Pliocene, UM: Upper Miocene, MM: Central Miocene, GrTf: Lower Miocene (Green Tough), PG: Paleogene, K: Cretaceous and thrust zone, B: Basement rock) (added epicenter to Fig. 18 of Yoshida et al., 2007).

ern stations (Atsuma Townhall, IBUH03, JMA Atsuma, HKD126) are characterized by a pulse-like wave with a period of about 2 –3 s at the beginning of the principal motions. On the other hand, the records of HKD128 and IBUH01, which are located in the north, are characterized by the short-period waves.

Acceleration response spectra (Fig. 7) of the southern four stations have peaks in the period of 2–4 s corresponding to the pulse-like waves, and the responses at the period longer than 1 s are comparable to the JR Takatori record of the 1995 Kobe earthquake. On the other hand, the response spectra of the HKD128 and IBUH01 have a peak at around 0.7 s and around 0.5 s, respectively, and the shape and level of the spectra are comparable to that of the JMA Kobe record of the 1995 Kobe earthquake. Since the ground motion of the HKD128 and the Atsuma Townhall are quite different in terms of frequency content and waveform characteristics while the two stations are located at a similar orientation from the epicenter and the epicentral distance differs by only about 5 km, it is reasonable to assume the subsurface structure around the two stations is very different.

The acceleration waveforms and acceleration response spectra for the stations in the east of the epicenter

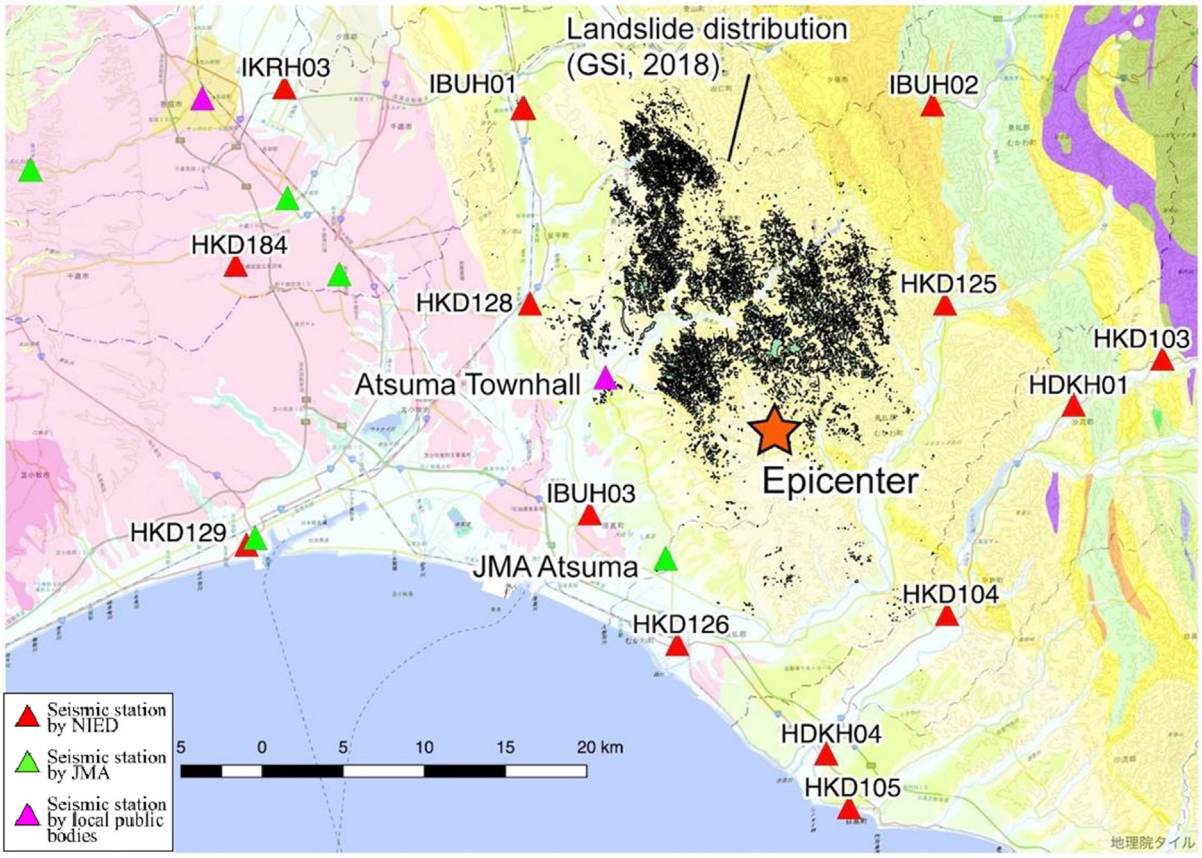

Fig. 5. Location of seismic stations in the epicentral area of the 2018 Hokkaido Eastern Iburi earthquake with landslide distribution (GSI, 2018) and geological map (Geological Survey of Japan/AIST, 2019).

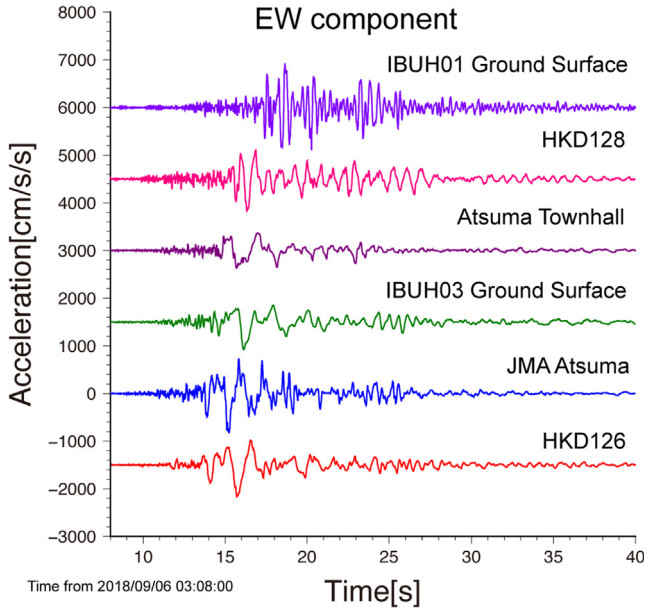

Fig. 6. Acceleration waveforms at seismic stations in the west of the epicentral area during the mainshock of the 2018 Hokkaido Eastern Iburi earthquake.

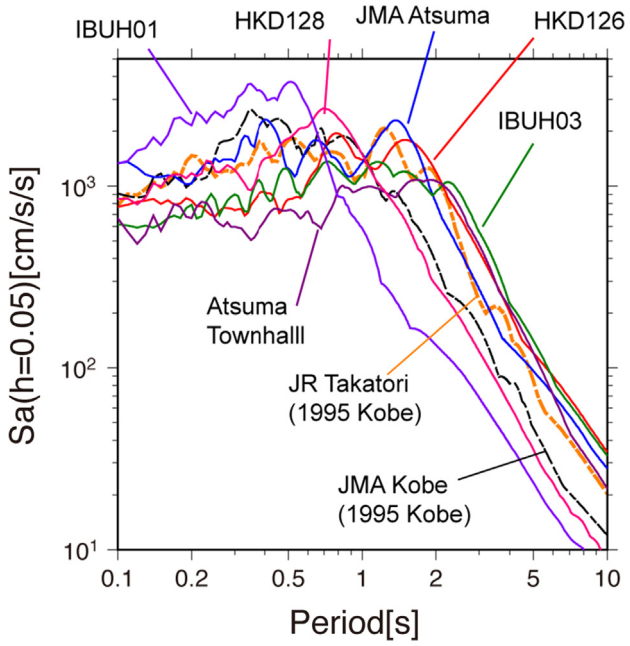

Fig. 7. Acceleration response spectra of the waveforms in Fig. 6.

(IBUH02, HKD125, HKD104, HDKH04) are shown in Figs. 8 and 9. For a comparison with the west, the record of the HKD126 is also shown. In general, the waveforms for these stations in the east of the epicenter are dominated by short-period waves with few long-period (longer than 1 s) waves. The ground motion in the area with a lot of

landslides (Fig. 5) is likely to have been characterized by short-period waves like those observed at IBUH01 and HKD125 because the recorded ground motions in the epicentral area were largely controlled by the subsurface structure, and the landslide area is located out of the Ishikari-Yufutsu basin.

1.3. Ground motion in the epicentral area and in Sapporo city

In this section, the ground motions of the 2018 Hokkaido Eastern Iburi earthquake around Sapporo city are compared with those of the 2003 Tokachi-oki (M 8.0) Earthquake. Fig. 10 shows the distribution of the seismic stations around Sapporo city. Seismic stations HKD180 and HKD182 were selected for the comparison because the ground motion records for the two earthquakes are easy to download and also because Kiyota-ward, where widespread liquefaction occurred, is between the two stations. Fig. 11 displays the waveforms and acceleration response spectra. The acceleration amplitude of the 2018 earthquake was more than twice that recorded in the 2003 earthquake. A comparison of the response spectra shows that the ground motions of the 2018 earthquake were at least twice as strong as those of the 2003 earthquake during the first 1 s, while after 2 s, the opposite was seen. When comparing the damage due to the 2018 earthquake around Sapporo city with that of the 2003 Tokachi-oki Earthquake, it is necessary to pay attention to the difference of the frequency contents of the ground motions as well as their amplitude and duration.

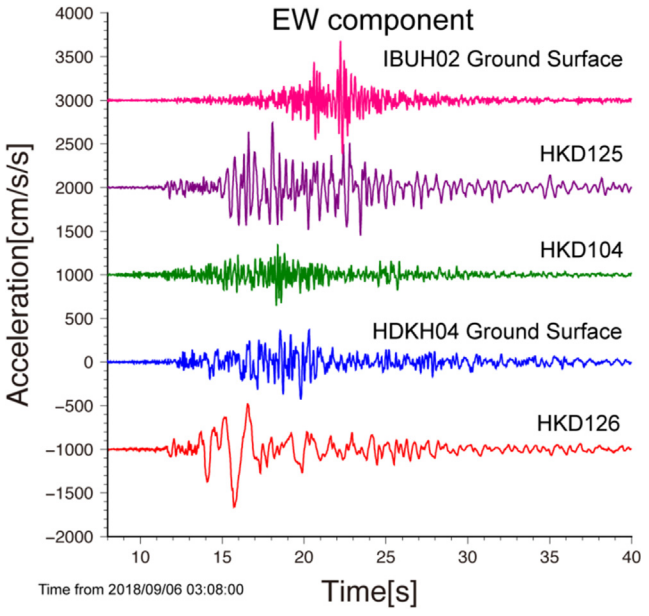

Fig. 8. Acceleration waveforms at seismic stations in the east of the epicentral area during the mainshock of the 2018 Hokkaido Eastern Iburi earthquake.

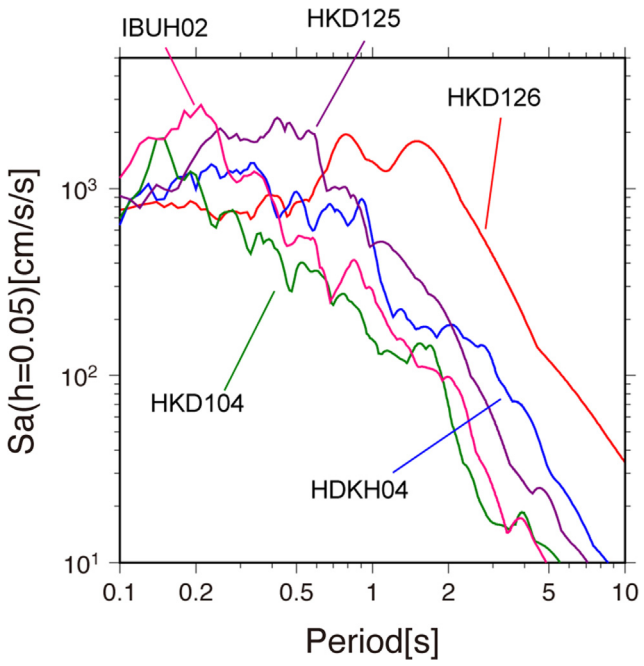

Fig. 9. Acceleration response spectra of the waveforms in Fig. 8.

2. Geotechnical damage caused by 2018 Hokkaido Eastern Iburi earthquake

2.1. Outline of geo-disasters due to 2018 Hokkaido Eastern Iburi earthquake

Ground deformation (including small-scale damage) associated with the 2018 Hokkaido Eastern Iburi earthquake occurred over a wide area, with damage confirmed at more than 400 locations. Since it was difficult for the JGS Survey Team to investigate all geo-disasters in detail during a short period of time, the investigation was limited to major geo-disasters with different damage mechanisms which occurred in central Hokkaido within a distance of approximately 80 km from the epicenter. For example, a large number of slope failures and landslides occurred on the hills covered with the volcanic pumice fall deposit layers in Atsuma and Abira, which were about 25 km from the epicenter (Fig. 12a, b), while severe liquefaction-induced ground deformation occurred in a residential area in Kiyota-ward, Sapporo, more than 50 km from the epicenter (Fig. 12c). It should be noted that while everywhere at the outer periphery of the Tomato-Atsuma Thermal Electric Power Plant located in Tomakomai near the epicentre experienced sand boiling at landfills, the uneven subsidence of road, and inclined sea revetment due to liquefaction (Fig. 12d), but little severe damages to the civil engineering facilities occurred inside the electric power plant. This is due to the countermeasures that had been taken against the liquefaction of the foundation. Among the geo-disasters investigated by the JGS survey team, the liquefaction-induced ground deformation in a residential

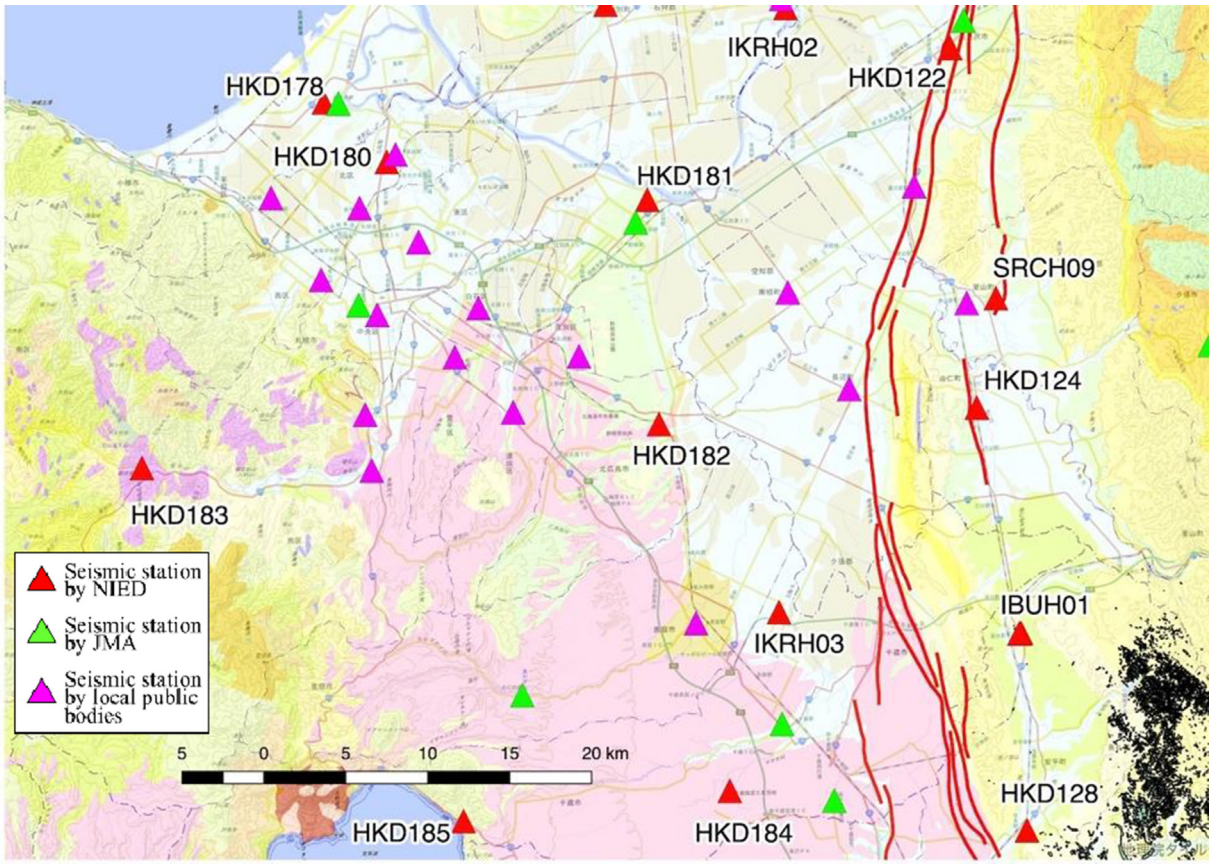

Fig. 10. Location of seismic stations around Sapporo City with landslide distribution (GSI, 2018) and geological map (Geological Survey of Japan/AIST, 2019).

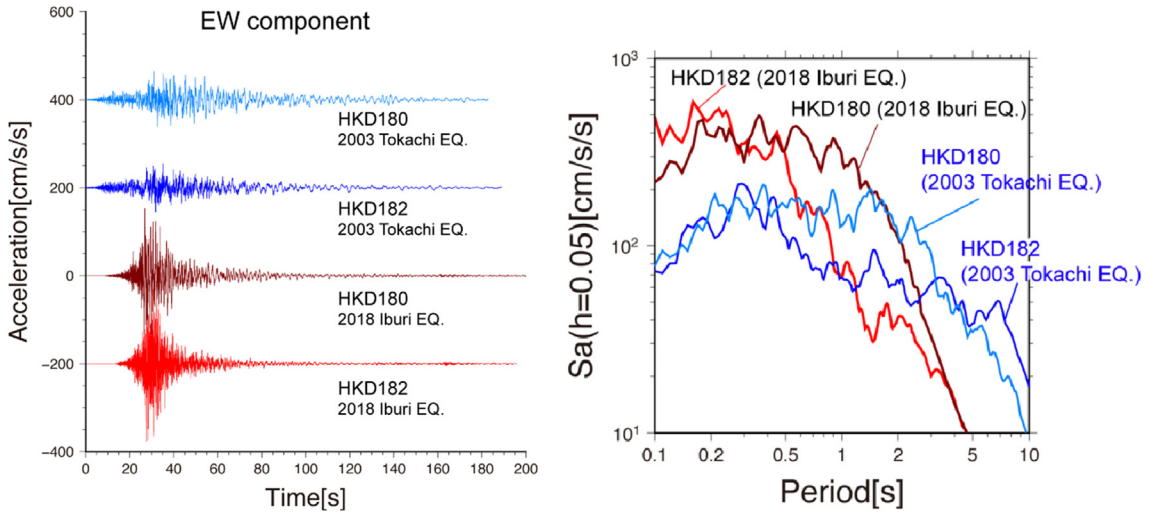

Fig. 11. Acceleration waveforms and acceleration response spectra of the 2018 Hokkaido Eastern Iburi Earthquake and the 2003 Tokachi-oki Earthquake at two observation points (HKD180, HKD182) around Sapporo City.

area in Sapporo, and the large-scale and wide-area swarm slope failures occurred at hill sides in Atsuma and Abira are considered to be examples of uncommon damage patterns rarely seen in earthquake disasters. Detailed information about these two distinctive geo-disasters caused by the 2018 Hokkaido Eastern Iburi earthquake can be found in Watabe and Nishimura (2020) and Kawamura et al. (2019). This section introduces another major geo-disaster where the JGS survey team conducted a detailed investigation into the causes and mechanisms.

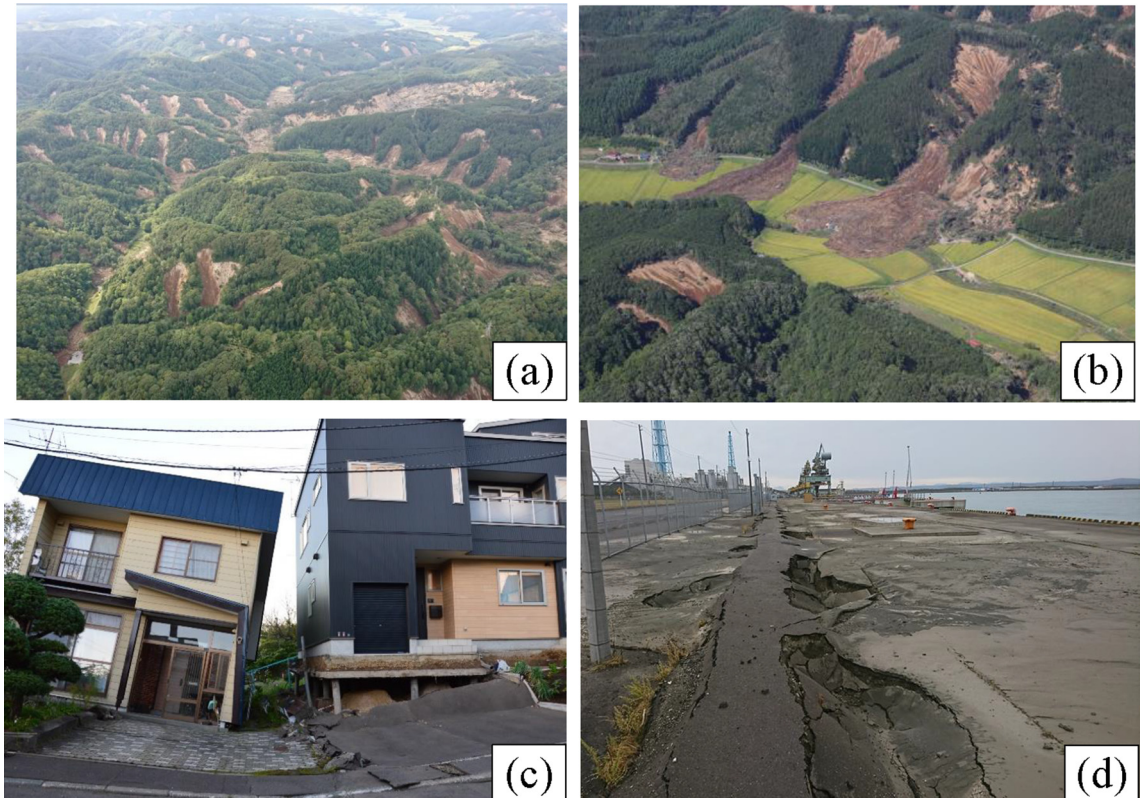

Fig. 12. Geotechnical damage caused by the 2018 Hokkaido Eastern Iburi Earthquake: (a) slope failures in Atsuma (Fig. 5), (b) slope failures with sediment flow in Atsuma (Fig. 5), (c) tilted house on the belt-shape depressed area due to liquefaction without sand boiling in Sapporo (Fig. 1), (d) uneven subsidence of road due to liquefaction with sand boiling in Tomakomai (Fig. 1): (a), (c), and (d) taken by Watabe, Y., Hokkaido Univ.; (b) provided from Japan Asia Group, PASCO Corporation.

Fig. 13. Survey points on road damage along the subway lines at the Kita ward and Higashi ward in Sapporo City.

2.2. Liquefaction induced settlement of the road above the subway line in Sapporo city

Severe liquefaction induced settlement of the road above the subway line was observed in the area around Kita 34 Station of the Namboku line in Kita-ward and the Higashi 15-chome Tonden street in Sapporo City after the earthquake, as shown in Fig. 13. A field investigation was conducted on September 8–9th 2018 corresponding to 2–3 after the earthquake.

(a) Namboku subway line at Kita-ward

Fig. 14 shows the closed-off sections near Kita 34 Station and the locations where settlement and depressions after the earthquakes were observed. Fig. 15 shows the situation after the earthquake, taken from the location of the numbers shown in Fig. 14. Two days after the occurrence of the earthquake, repair work had already started on the road above the Namboku subway line, and a prompt response was being implemented for emergency restoration. On the other hand, as shown in the picture taken from No. 3, although slight deformation was seen on the foundation tiles of the building facing Sapporo Shindo drive, no noticeable damage was seen in Sapporo Shindo drive or to the sidewalks. Thus, it was found that the damage was concentrated on the road above the Namboku subway line.

Fig. 16 shows the geological columns around the affected area obtained from the Geological and Geotechnical Information Database G-Space II in Japan. From this figure, it can be seen that the original ground around Kita 34 Station is mainly composed of clay and silt with a very small N value and sand with an N value of 10 or less, partially containing organic soil. Moreover, the groundwater level at the time of the earthquake occurrence is unknown, but in the geological column map, the groundwater level is at a depth of 1.0–3.0 m from the ground surface.

(b) Toho subway line at Higashi-ward

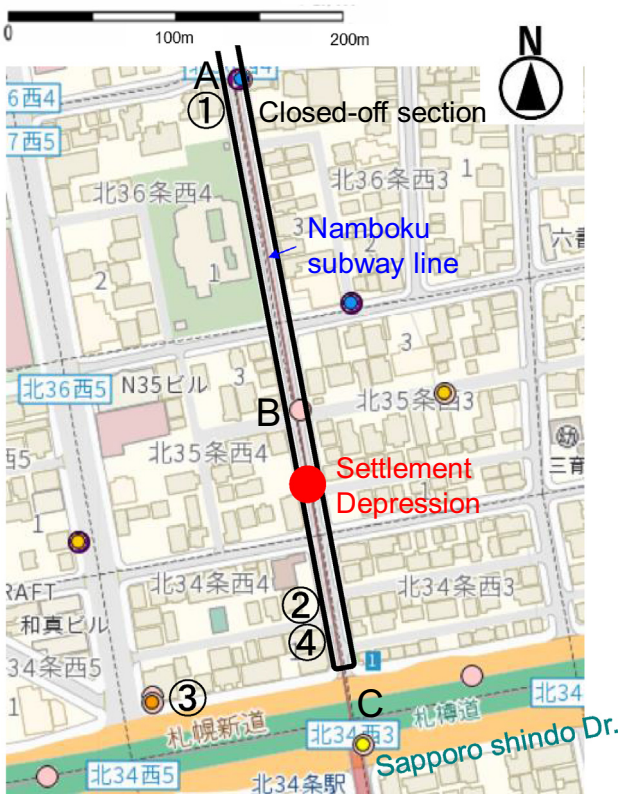

Fig. 14. Closed-off section and damage situation around Kita 34 station of Namboku subway line in Kita ward, Sapporo with the map by G-Space II.

Fig. 15. Damage situation near Kita 34 Station two days after the earthquake (photo locations referred to Fig. 14).

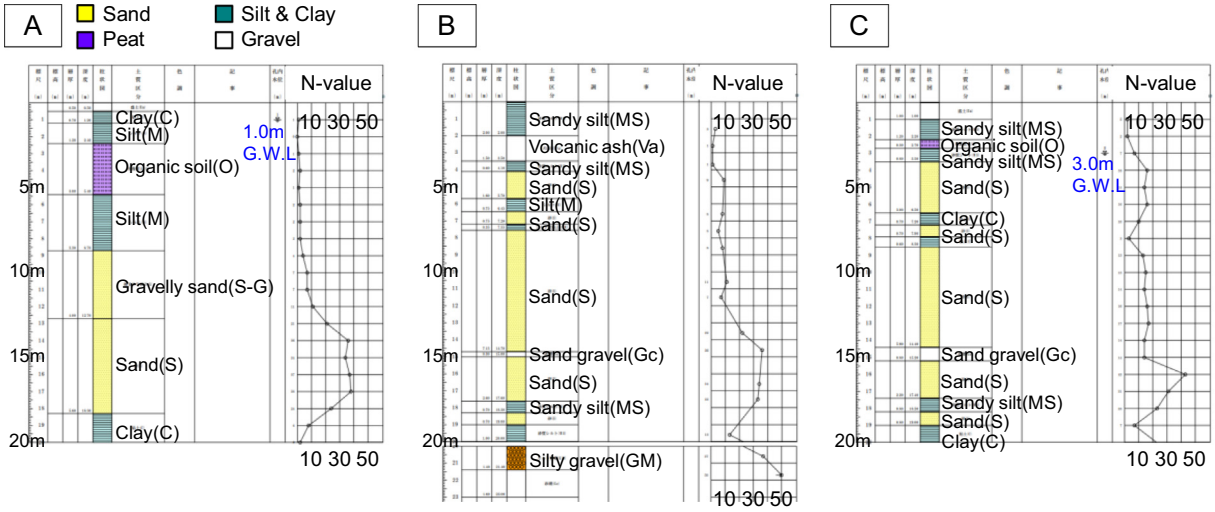

Fig. 16. Geological column diagram of the original ground around Kita 34 Station based on G-Space II.

The damage situation in Higashi 15-chome Tonden Street above Toho subway line is shown in Fig. 17. In Higashi 15-chome Tonden Street, the road was damaged by liquefaction-induced settlement over about 4.4 km north to south around Kita 13 to Kita 47, and was closed except for some intersections. Temporary restoration started on the 7th of Sep. which is the day after the earthquake, and traffic was resumed sequentially as the temporary restoration was completed for each section, and full passage was possible around 5 pm on the 17th of Sep.

Fig. 18 shows the situation after the disaster at the location of the numbers shown in Fig. 17. Kita 47 to Kita 42 (Sakaemachi Station), which is the northernmost point in the damaged area of Higashi 15-chome Tonden street, experienced the most significant damage, with large-scale road settlement. As shown in Fig. 18 ⑤ and ⑥, up to about 1 m of road settlement and exposure of the buried structure were observed. In addition, the settlement and depressions of not only the driveway but also the sidewalk could be confirmed. The road depressions were concen-

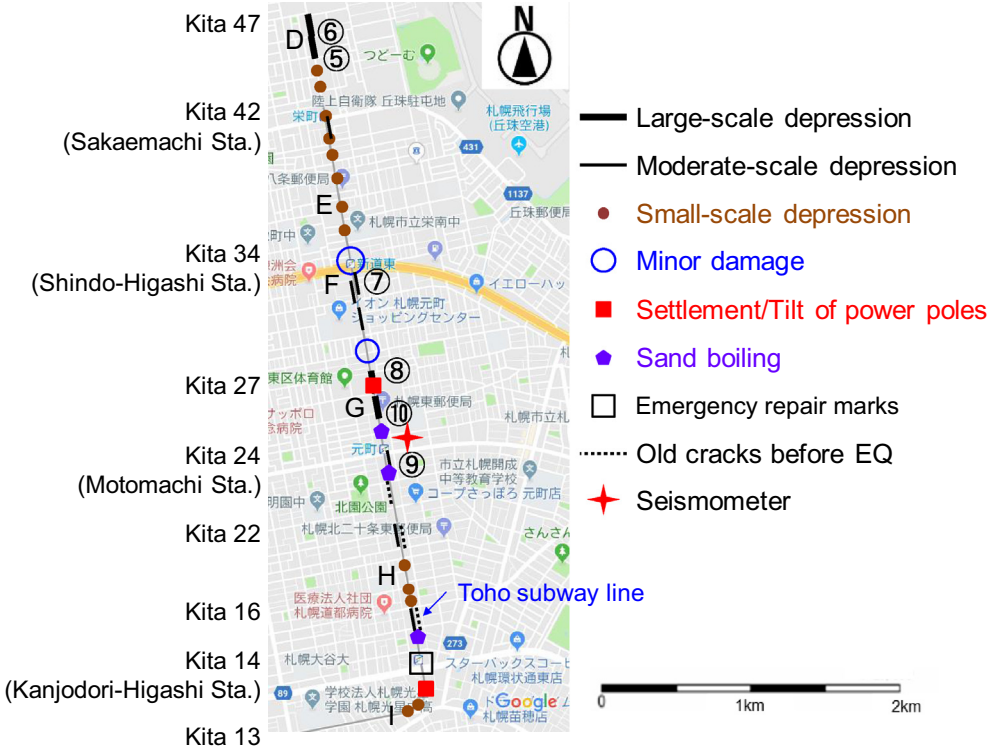

Fig. 17. Damage to Higashi 15-Chome Tonden Street with the map by Google.

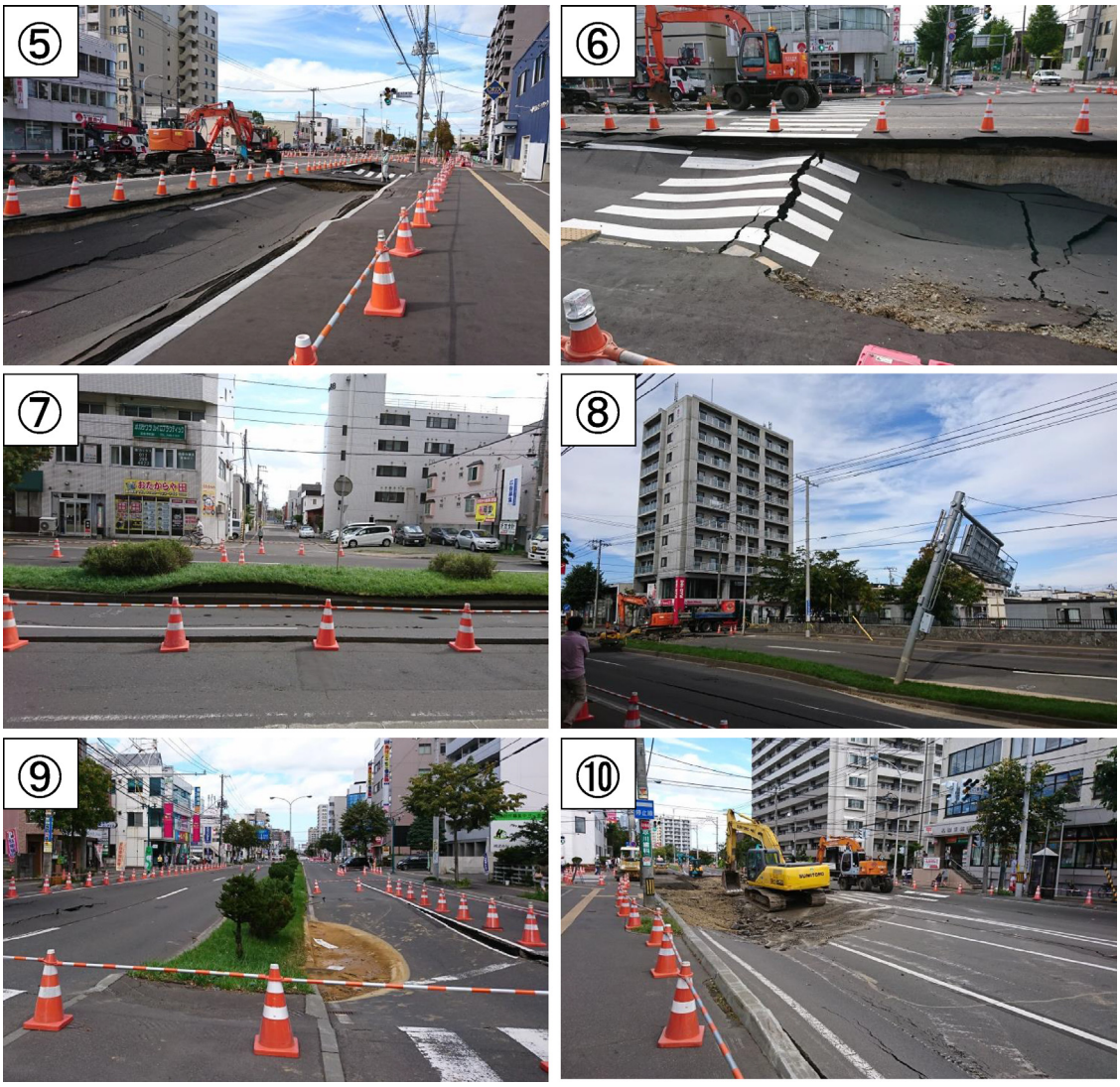

Fig. 18. Damage situation along Higashi 15-Chome Tonden Street two days after the earthquake (photo locations referred to Fig. 17).

trated on the Toho subway line, since the location corresponds to the location of the sidetrack of the Toho subway line.

From Kita 42 (Sakaemachi Station) to Kita 35 a small-scale road settlement occurred. Traffic was controlled at the intersection of Kita 42 (Sakaemachi Station) ~~was out of traffic control~~, but the scale of damage was less than the situation of the northern area.

From Kita 34 (Shindo Higashi Station) to Kita 27, settlement of the road occurred near the median, and long cracks occurred along the settlement along the road as shown in Fig. 18 ⑦.

From Kita 27 to Kita 22 including Motomachi station, the occurrence of large-scale road collapse and the inclination of road signs was observed along with sand boiling, suggesting that liquefaction occurred. Also in the area, a seismic intensity of 6 or less was observed with a seismograph installed at the Higashi fire department of Sapporo City. This was the largest seismic intensity in Sapporo city.

From Kita 22 to Kita 16, the occurrence of small-scale road settlement and sand boiling were observed, suggesting that liquefaction occurred. Repair marks for old cracks were found in the area, and it is considered that road deformation had occurred before the earthquake.

From Kita 16 to Kita 13 including Kanjodori-Higashi station, along the Toho subway line alignment, the occurrence of settlement or deformation of the road was observed from north-south direction to east–west direction. In addition, it was confirmed that emergency restoration was already completed on the sidewalk near Kanjodori-Higashi Station.

Along Kita 13 Kitago Street, although there is a repair mark of the pavement implemented before the earthquake between Higashi kuyakusho mae Station and Kita 13 Higa-

shi Station, there are only two repair marks after the earthquake. It was found that the damage was minor compared to that at Higashi 15-chome Tonden street.

According to the Sapporo City High Speed Toho Subway Line construction history (between Sakaemachi and Hosui-Susukino) published by the Sapporo City Transportation Bureau Planning Department in 1989, in the 1970s to 1980s the Toho subway line was constructed by the open-cut method using underground continuous walls and muddy water solidified walls: these were the latest technique at that time. According to records, clean sand which was purchased for backfill soil was used. It can be inferred that the backfill soil was liquefied, and that the damage due to ground subsidence and road collapse was the result of this liquifaction. Figs. 19 and 20 show schematic longitudinal and geological profiles along the Toho subway line described in the same document. Here, *H* in Fig. 19 is the soil thickness at the center of the subway station, and the values on the subway line are the longitudinal grades. In the damaged area along Higashi 15-chome Tonden Street, peat and corroded soil layer with a layer thickness of 1–3 m exists near the ground surface, the cohesion soil layer and the sandy soil layer alternate, and the gravel layer which is assumed to be bearing layer deposits below them. Along Kita 13 Kitago street, peat and corroded soil layer with a layer thickness of 1–3 m exists around 7–10 m from the ground surface below the alternative layers of cohesive soil and sandy soil. The gravel layer is deposited below it. In addition, the ground surface slopes gently toward the Sea of Japan, and the soil thickness of backfill soil reaches 9.3 m at Sakaemachi Station with the increase of the soft layer thickness. In addition, a sewage duct of 3.8 m × 3.1 m and a sewage pipe with a diameter of 800–2000 mm are buried along Higashi 15-chome Tonden street in the affected area. There is a construction record that an air mortar was filled between the subway structure and the retaining wall (25 cm) at the intersection with the main drive where only minor damage were observed. Based on the above, it is possible that the compaction of the backfill soil in the vicinity of the buried structure and between the subway structure and the retaining wall was insufficient.

Fig. 21 shows the geological columns around the affected area obtained from the Geological and Geotechnical Information Database G-Space II in Japan,

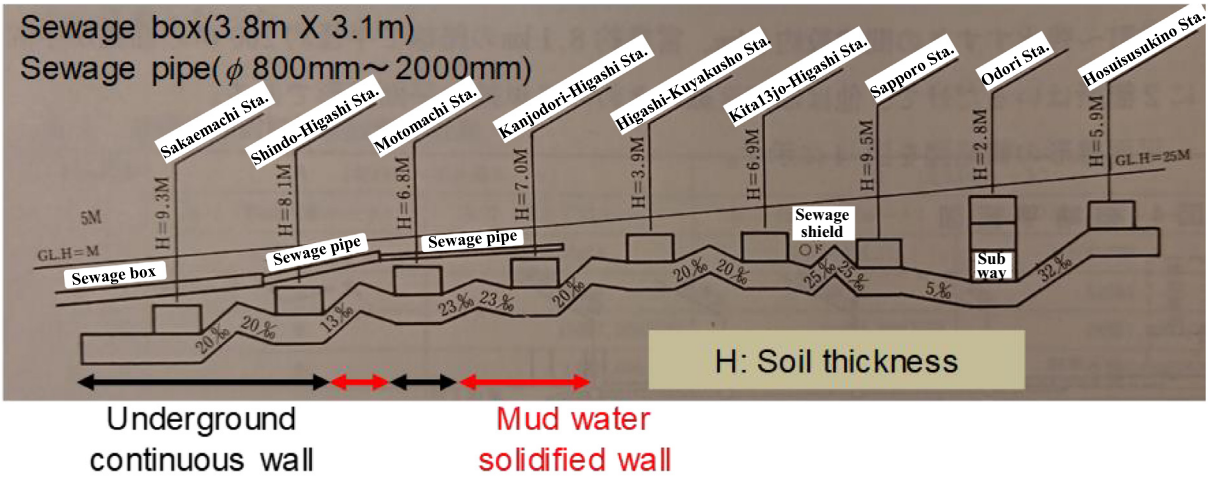

Fig. 19. A schematic longitudinal profiles along the Toho subway line drawn in the reference (Sapporo City Transportation Bureau Planning Department, 1989).

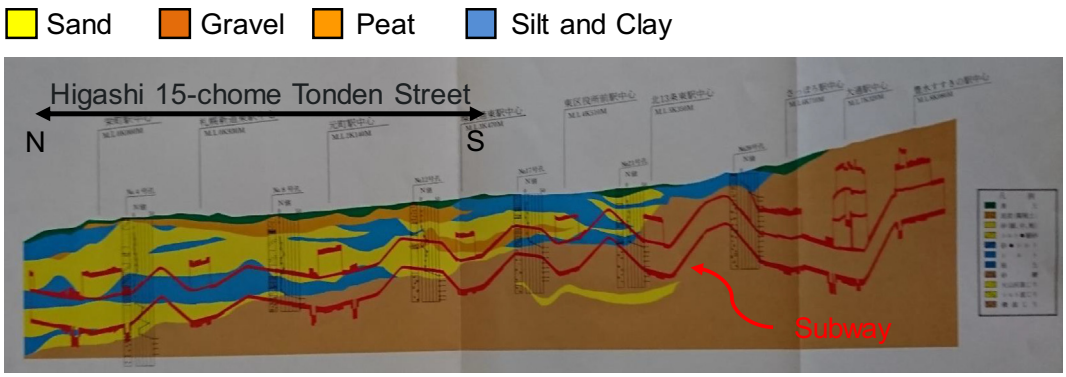

Fig. 20. A schematic longitudinal and geological profiles along the Toho subway line drawn in the reference (Sapporo City Transportation Bureau Planning Department, 1989).

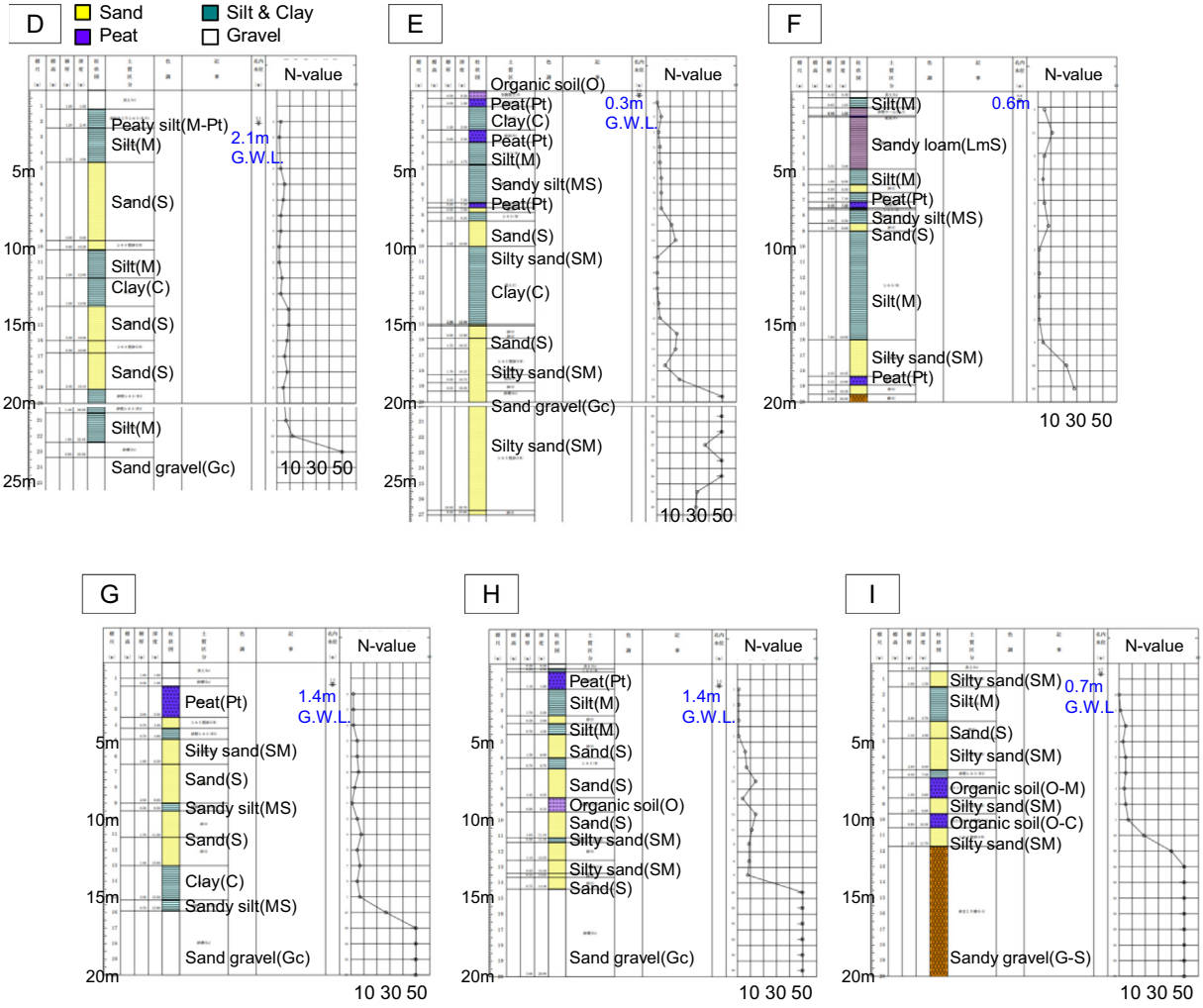

Fig. 21. Geological column diagram of the original ground along Higashi 15-chome Tonden street based on G-Space II.

showing the location in Fig. 17. It was found that the original ground around this area partially contained organic soil, clay and silt with very a low N value and sand with an N value of 10 or less are deposited to a depth of 15–20 m as the same as the schematic longitudinal and geological profile. From Kita 34 (Shindo Higashi Station) to Kita 22, thick layers of peat and organic soil are deposited up to about 3 m near the ground surface. The original ground around Kita 16 to Kita 13 and along Kita 13 Kitago Street also partially contained organic soil, clay and silt with a very low N value and sand with an N value of 10 or less are deposited to a depth of 10 m. This is less than that at the northern part. In addition, the peat and organic soil layers are deposited about 2 m around 7–10 m from the ground surface, indicating that the deposition is shallower than in the northern area. Moreover, the groundwater level at the time of the earthquake occurrence is unknown, but in the geological column map, the average groundwater level is approximately 2.0 m from the ground surface. It tends to decrease toward the Sosei River, which flows north and south on the west side of this area.

(c) Summary

The road settlement damage in Kita-ward and Higashi-ward is distributed along the subway line and there are scattered traces of sand boiling around these areas. It is thought that the backfill soil (purchased clean sand) which was used for the subway construction with the open-cut method liquefied and the road settlement was induced. Based on the geological column diagrams near the affected area, it is composed of a soft sandy ground with N value 10 or less or a clay/silt with N value 4 or less and an organic soil including peat layer, which depth is up to about 10–15 m. The largest seismic intensity observed in Sapporo city was 6 lower on the JMA seismic intensity scale of seven at the Higashi fire station, indicating that that the seismic response may have been amplified and liquefaction may have been promoted in this area. In the areas with severe settlement (around Sakaemachi Station and Motomachi Station), the soft ground is thick, with a large cutting depth and thick backfill soil. Thus, it would appear highly likely that there is a strong correlation between the backfill soil

thickness and the scale of the damage. In addition, the groundwater level, at a depth of less than 3 m from the ground surface, is likely to have created an elevated risk of liquefaction. Also, according to construction records, an air mortar fill was used between the subway structure and the retaining wall (25 cm) at the intersection with the main drive where only minor damage were observed. Based on the above, it is reasonable to conclude that compaction of the backfill soil in the vicinity of the buried structure and between the subway structure and the retaining wall was insufficient.

3. Lessons from geotechnical damage caused by 2018 Hokkaido Eastern Iburi earthquake

In order to promote the academic research of the phenomena and causes of geo-disasters induced by a massive earthquake in Hokkaido, and the improvement of disaster prevention/mitigation technologies, this section summarizes the specific characteristics of the geo-disasters caused by the 2018 Hokkaido Eastern Iburi earthquake, and the lessons confirmed in the geo-disasters, in terms of two distinctive phenomena, namely liquefaction and slope failure. First, in the case of liquefaction damage, there are three important technical considerations:

(1) Influence of seismic motion characteristics on liquefaction damage

Liquefaction damage was observed in the wake of the 2018 Hokkaido Eastern Iburi earthquake as well as after the 2003 Tokachi-oki earthquake. However, the damage due to liquefaction differed in these two earthquakes. As explained in the previous section, ground motion in Sapporo city during the 2018 Hokkaido Eastern Iburi earthquake was stronger than that of the 2003 Tokachi-oki earthquake during the first second, but weaker in the longer period range. It is considered that such differences in the seismic motion characteristics induced different types of liquefaction damage. Therefore, the influence of seismic motion characteristics on liquefaction damage should be examined in detail.

(2) Liquefaction risk of age-deteriorated residential land embankments under climate change

Another likely reason for the difference in the damage situation due to liquefaction between two severe earthquakes in 2013 and 2018 is the change over time in weather and ground conditions. In the site investigations by the JGS survey team (JGS, 2019), rainfall of about 30 mm/day was reported before the earthquake and the resulting liquefaction. According to measurement records (Sapporo, 2019), ground water levels in Sapporo city have shown a gradual increase in some places over recent years. Besides, degradation to the drainage facilities inside the soil attached to the earth structures, like embankment, may have occurred over time due to the deterioration of drainage function by the clogging and/or the cracking. These groundwater level rising factors may have resulted in an increased risk of liquefaction during an earthquake. Therefore, in the case of significant change in the in the surrounding environment conditions from the design conditions with the passage of time since the construction of earth structures, it is necessary to monitor the geotechnical conditions around the earth structures, and reconsider disaster prevention/mitigation measures for the specific conditions at those locations.

(3) Influence of topographic factors and soil characteristics on liquefaction damage

Many local governments in Japan have created and published a liquefaction hazard map for the area around their residence. Fig. 22 compares the liquefaction-damaged areas by the 2018 Hokkaido Eastern Iburi earthquake with the liquefaction hazard map made by Sapporo City (Sapporo, 2018). In this figure, the observed damaged areas are mainly classified into the area with the "Highest possibility of liquefaction" and four risk levels are included in the liquefaction hazard map of Sapporo City. This confirms the usefulness of this liquefaction hazard map.

However, although the risk of liquefaction is well captured, the risk of damage cannot be inferred from this map. In fact, as a result of this earthquake, depending on the thickness and distribution (inclination) of the liquefaction layer, the groundwater level, the depth at which liquefaction occurred from the ground surface, and the characteristics of the liquefied soil, the liquefaction damage was remarkably different, even between Kiyota ward (Fig. 12c) and Kita ward/Higashi ward (Figs. 15 and 19), or within Kiyota Ward (JGS, 2019). Therefore, it is necessary to realize that the damage caused by liquefaction is likely to be different even when the risk of liquefaction is at the same level in the liquefaction hazard map. After conducting a detailed ground survey in consideration of topographical and ground information (e.g. the boundary between cut slope and embankment), disaster prevention/mitigation measures should be taken assuming the damage mechanism according to the ground conditions.

Next, as for the slope failure damage, there are three important technical consideration items:

(1) Prevention and mitigation methods for seismic motion beyond expectation

At the mountains and hills in the Atsuma River basin where a large number of slope failures and landslides occurred, multiple layers of volcanic pumice fall deposits with different eruption periods mainly originating from Tarumae volcano, Eniwa volcano, and Shikotsu volcano are widely distributed on sedimentary rocks. Among these, the Shikotsu pumice fall deposit (Spfa-1) erupted from the Shikotsu caldera about 46,000 years ago, and the Eniwa

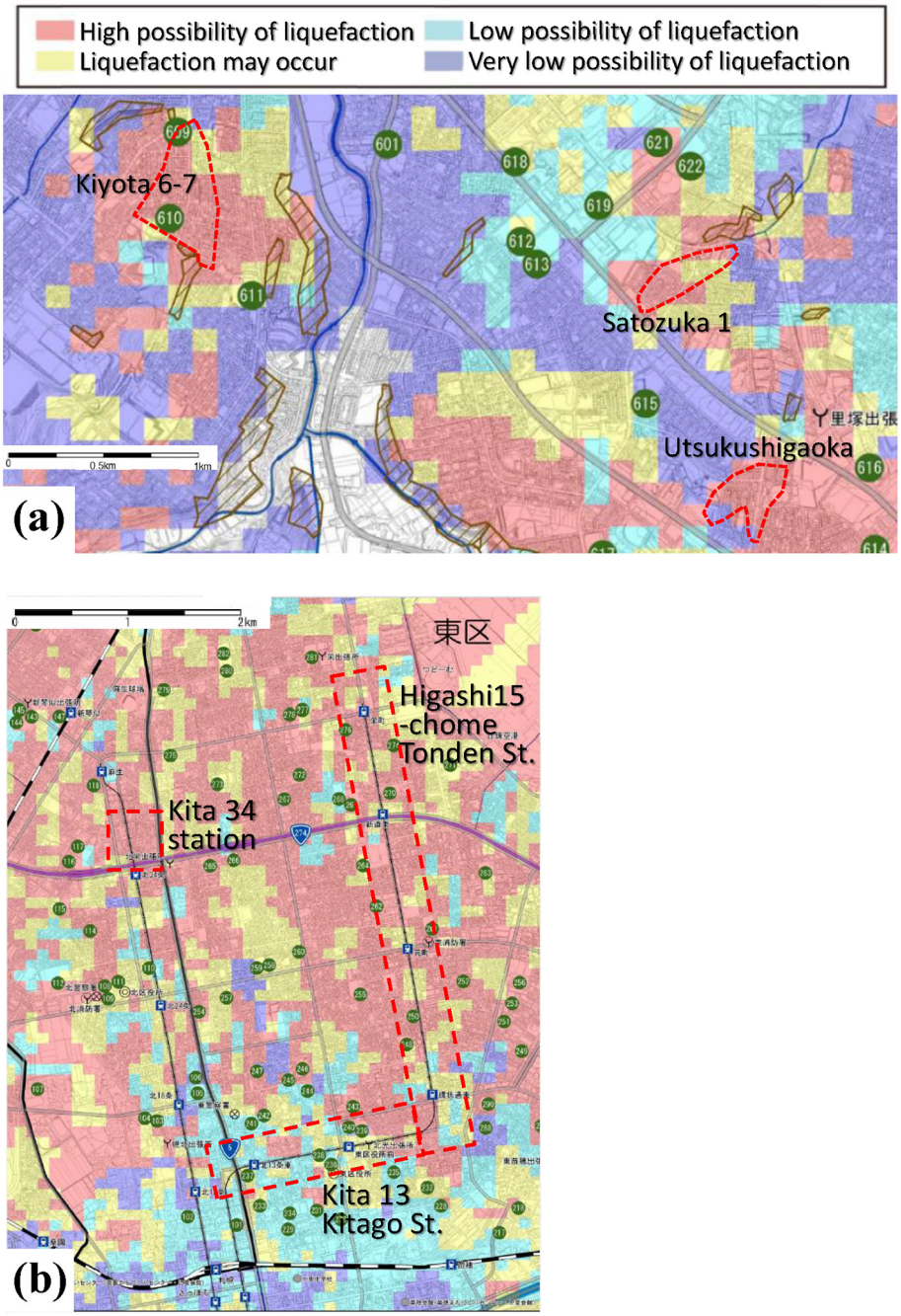

Fig. 22. Liquefaction hazard map for Sapporo City (Sapporo, 2018) with liquefaction-damaged areas by the 2018 Hokkaido Eastern Iburi earthquake: (a) Kiyota ward, (b) Kita ward and Higashi ward.

pumice fall deposit (En-a) erupted from the Eniwa volcano about 20,000 years ago. Four kinds of pyroclastic fall deposits erupted from the Tarumae volcano (Ta-d, Ta-c, Ta-b, and Ta-a) about 9000 years ago, about 2000 years ago, in 1667 CE, and in 1739 CE, respectively. By observing the stratigraphic structures at many slope failure sites (Fig. 23), little disorder of the strata due to crustal movement and landslides was observed. This means that slope failures due to large earthquakes with the same magnitude as the 2018 Hokkaido Eastern Iburi earthquake have not occurred for a long time. Fig. 24 compares the slope collapse locations at the 2018 Hokkaido Eastern Iburi earthquake and the sediment disaster warning areas due to heavy rainfall in Atsuma. Though the latter partly overlap with the former, regrettably it is not appropriate to use the map for sediment disaster warning areas as the risk assessment of slope failure during an earthquake. Therefore, it is necessary to discuss and to propose new prevention and

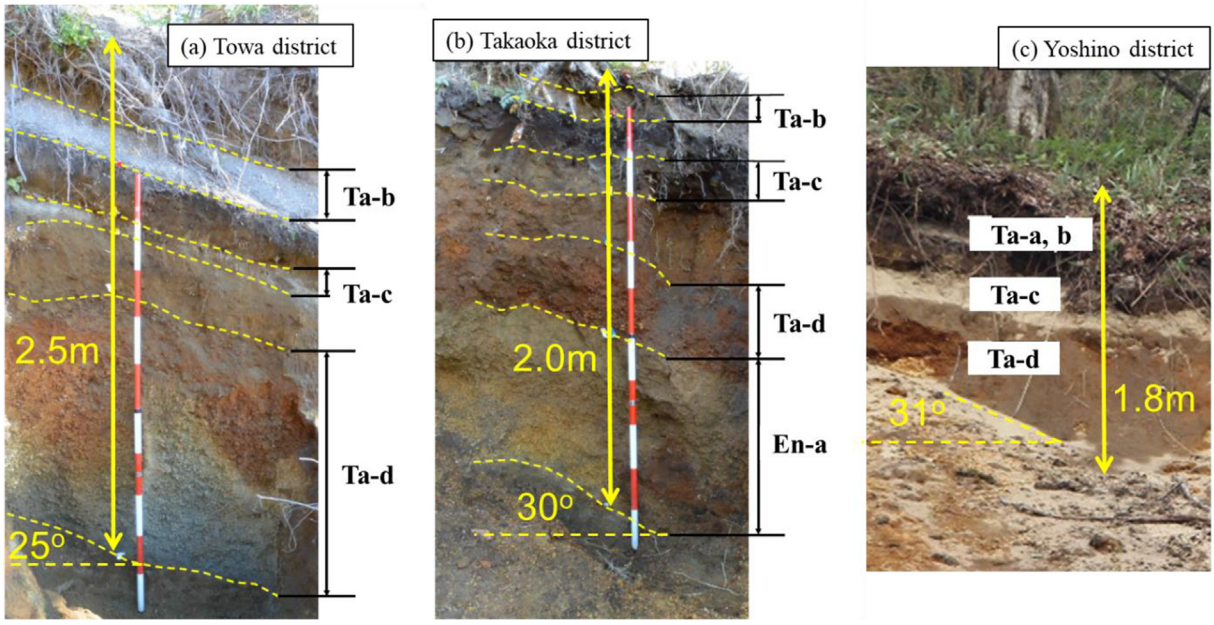

Fig. 23. Stratigraphic situations at slope failure sites in Atsuma: (a) Towa district, (b) Takaoka district, (c) Yoshino district (locations of each district referred to Fig. 24).

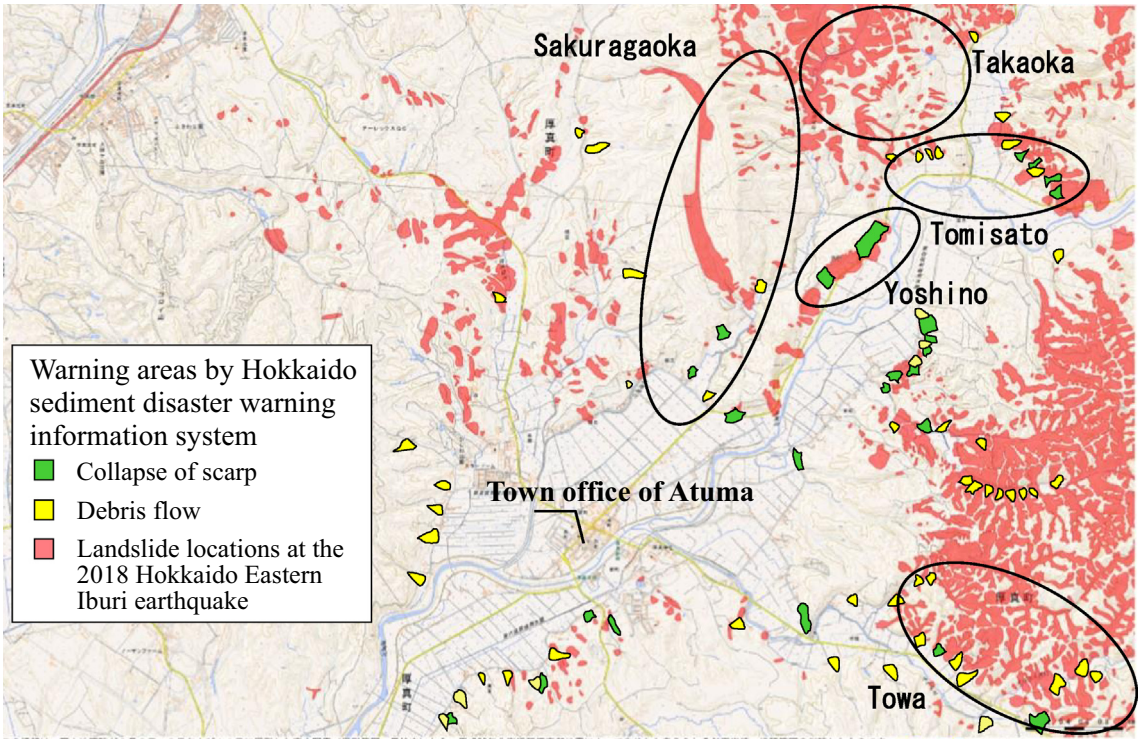

Fig. 24. Comparison the landslide locations at the 2018 Hokkaido Eastern Iburi earthquake (GSI, 2018) with the sediment disaster warning areas in Atsuma (Hokkaido, 2018b).

mitigation measures for geo-disasters against earthquake motion beyond expectations keeping in mind that past experiences are not useful indicators.

(2) Causes for variation in the occurrence of slope failures depending on location

Within about 25 km from the epicenter (Fig. 5), the slope collapses were mainly distributed in the north epicentral areas, like Atsuma and Abira. Variations in the damage situation of slope failures are considered to be due to the following two reasons. One factor is the difference in the characteristics of seismic motion near the epicenter

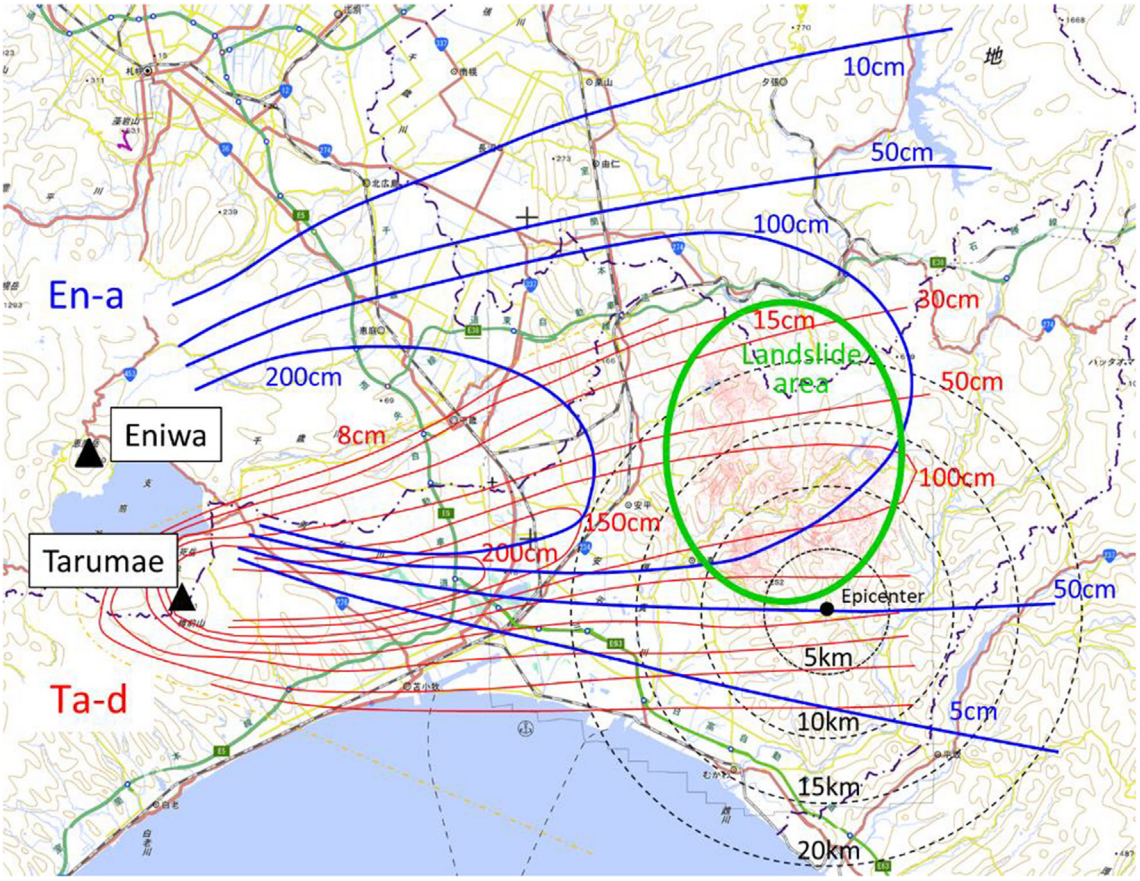

Fig. 25. Distribution area and thickness of pyroclastic fall deposits from Tarumae and Eniwa volcanos with landslide distribution (GSI, 2018).

depending on the amplification and attenuation characteristics of soil ground during earthquake motion propagation. As shown in Figs. 6–9, there are two types of measured ground motion, namely a pulse-like wave with a period of about 2–3 s at the beginning of the principal motions, and then short-period wave without long-period (longer than 1 s) components. The former acceleration waveform was observed at the southern part of epicentral area, while the latter was observed at the north part. It is noted that these two areas seem to be divided by the subsurface structure boundary as shown in Fig. 5, and that multiple slope failures occurred in the north part of the subsurface structure boundary. Therefore, it can be said that the amplification and attenuation characteristics of soil ground during earthquake motion propagation have a significant influence on the risk of earthquake-induced slope failures.

The other factor is the difference in the deposition status of volcanic pumice fall deposits depending on the distance and direction from the eruption source. Fig. 25 shows the distribution area and thickness for two kinds of the pumice fall deposits which erupted from the Tarumae volcano (Ta-d) and the Eniwa volcano (En-a), respectively. The total thickness of En-a and Ta-d is approximate 100–200 cm at the slope failure locations in Atsuma town, while the thickness is thinner at the area where little slope failure was seen. From these facts, it is obvious that many slope failures occurred in the distribution area with thick pyroclastic deposits. When conducting the slope stability analysis under the assumed calculation conditions shown in Fig. 26 by referring to Amemiya (2019), the depth of the slip surface of the collapsed slope with a 25–35 deg range in the slope angle, which were frequently observed in Atsuma town, is between 1.5 m and 3.5 m. According to an estimation by the Ministry of Land, Infrastructure, Transport and Tourism (MLIT, 2018), the scale of slope collapses due to the 2018 Hokkaido Eastern Iburi earthquake was as follows: (a) the amount of collapsed sediment: 30.0 million m^3; (b) the collapsed area 13.4 km^2. The average collapse depth estimated from the amount of collapsed sediment and the collapse area is about 2.2 m. In addition, according to the results of field investigation, though the slip surface position varied depending on the location, in most cases the collapse depth was approximately 2–3 m in places where Ta-d and En-a are deposited. From these results, it is recognized that the depths of all the slip surfaces was similar, indicating that the slope failures seen around Atsuma town were strongly influenced by the geological structures. Therefore, it is necessary to discuss and to propose prevention and mitigation measures

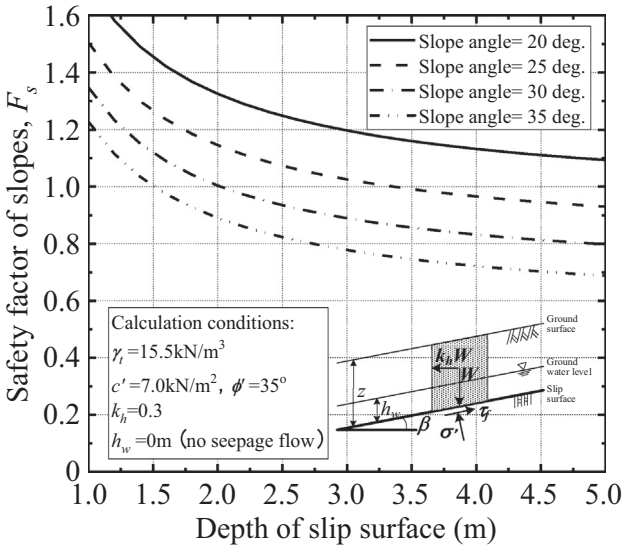

Fig. 26. Results of slope stability analysis: depth of slip surface for the collapsed slopes under various slope angles.

for earthquake-induced slope failures by considering both the amplification-attenuation characteristics of the local site and the geological structures.

(3) Influence of particle crushability and weathering degradation of volcanic soils on slope failures

CNHR (2019) reported that most of the slope failures induced by rainfall occur on slopes with a slope of 30 deg or more, but in the 2018 Hokkaido Eastern Iburi earthquake, slope failures occurred frequently even on relatively easy slopes with a slope of 30 deg or less. It was also reported that the moving distance of sediment flow caused by this earthquake was longer than the slope failure caused by rainfall. According to Kawamura et al. (2019), one of the causes for these phenomena, based on a series of laboratory element tests for weathered pyroclastic fall deposit (Ta-d), was that with the progressing weathering degree of volcanic soil, the particle crushability and the water retentivity increase and the shear strength decreases, resulting in a decrease in slope stability. For example, the slope failures with long-distance sediment flows shown in Fig. 12b were observed in some districts of Atsuma town, which is considered to be partly due to the special characteristics of the weathered crushable volcanic soil in addition to rainfall of Typhoon Jebi (T1821) which hit Hokkaido just before this earthquake. Besides, Amemiya (2019) explained that one of the causes of the long-distance sediment flow was particle breakage due to cyclic shearing during earthquake followed by the increase in the water content by pore water leaked from the intro-voids of crushed particles at the slip surface. These indicate that the earthquake-induced slope failures occurred in the area beyond the yellow zones in the sediment disaster hazard area designated by the Sediment Disaster Prevention Act under some special conditions that have yet to be considered. Therefore, it is necessary to discuss the designation of the sediment disaster hazard areas for earthquakes which differ from the rainfall-induced geo-disasters, taking into account the peculiarity of the material properties of crushable weathered volcanic soils specific to Hokkaido.

These are important research issues in considering the future path of geotechnical engineering and geo-disaster prevention/mitigation administration considering the regional characteristics of Hokkaido. The importance of these issues was brought to light after investigating the particular characteristics of the damage caused by the 2018 Hokkaido Eastern Iburi Earthquake. In order to promote disaster prevention and mitigation measures of civil engineering structures with a long service lifespan against massive earthquake-induced geo-disasters never experienced before, it is necessary to continue efforts to make corrections in the framework of the above-mentioned research issues while sharing a sense of crisis throughout society. In this case, particularly, it is essential to quickly establish a framework in which the industry, government, and academia can address the technical and social issues related to the prevention/mitigation of geo-disasters caused by strong ground motion. In the future, it is expected that specific measures will be drafted and implemented while incorporating the suggestions and recommendations of this report using an appropriate combination of hard and soft countermeasures.

Acknowledgments

We used K-NET, KiK-net records. We thank for JMA and Hokkaido prefecture for providing the seismic motion records at Atsuma Townhall and JMA Atsuma station. The authors sincerely acknowledge all those who provided "JGS Survey Team for Geotechnical Disasters in Hokkaido, Japan Induced by the 2018 Hokkaido Eastern Iburi Earthquake" with valuable information and research support, particularly the Hokkaido Regional Development Bureau, the Ministry of Land, Infrastructure, Transport and Tourism and the Hokkaido Government, and Hokkaido prefecture, Sapporo city, and Atsuma town.

References

Amemiya, K., 2019. Rapid landslide organization in earth (detritus) and the stability by Hokkaido Iburi Eastern Earthquake. In: Proceedings of the 2019 Research Presentation for Hokkaido Branch of Japan Landslide Society, pp. 39–42. (in Japanese).

Cabinet Office, 2019. Damage situation related to the 2018 Hokkaido Eastern Iburi Earthquake. (in Japanese) http://www.bousai.go.jp/updates/h30jishin_hokkaido/index.html.

Center for Natural Hazards Research, Hokkaido University, 2019. Symposium for looking back on the 2018 Hokkaido Eastern Iburi Earthquake and considering future disaster mitigation and reconstruction. (in Japanese).

Earthquake Research Committee, 2018. Headquarters for Earthquake Research Promotion, Evaluation of the 2018 Hokkaido Eastern Iburi

Earthquake. (in Japanese). https://www.static.jishin.go.jp/resource/monthly/2018/20180906_iburi_3.pdf.
Geological and Geotechnical Information Database G-Space II in Japan: https://www.gspace.jp/.
Geological Survey of Japan (GSJ), National Institute of Advanced Industrial Science and Technology (AIST), 2019. 1:200,000 scale seamless geological map V2. https://gbank.gsj.jp/seamless/index_en.html?.
Geospatial Information Authority of Japan (GSI), 2018. Map of the slope failure and sedimentation distribution due to the 2018 Hokkaido Eastern Iburi earthquake. (in Japanese).
Hokkaido, 2018a. Major earthquake damages in each area in Hokkaido occurred in the past. (in Japanese). http://www.pref.hokkaido.lg.jp/kn/ksd/jisshinhigai.htm.
Hokkaido, 2018b. Hokkaido sediment disaster warning information system. (in Japanese).
Japan Meteorological Agency (JMA), 2019. Seismic Intensity database.
Japanese Geotechnical Society (JGS) Survey Team for Geotechnical Disasters in Hokkaido, Japan Induced by the 2018 Hokkaido Eastern Iburi Earthquake, 2019. Reconnaissance report on geotechnical damage caused by the 2018 Hokkaido Eastern Iburi Earthquake. (in Japanese).
Kawamura, S., Kawajiri, S., Hirose, W., Watanabe, T., 2019. Slope failures/landslides over a wide area in the 2018 Hokkaido Eastern Iburi Earthquake. Soils Found.
Kurahashi, T., Ito, Y., Yamazaki, S., 2019. Damage of the 2018 Hokkaido Eastern Iburi Earthquake. In: Proceedings of annual the 2019 Japanese Landslide Society Hokkaido Branch, pp. 13–16. (in Japanese).
Ministry of Land, Infrastructure, Transport and Tourism (MLIT), 2018. Comparison of collapsed area at the 2018 Hokkaido Eastern Iburi Earthquake and past earthquake disasters. (in Japanese). https://www.mlit.go.jp/river/sabo/h30_iburitobu/181005_sediment_volume.pdf.
National Research Institute for Earth Science and Disaster Resilience (NIED), 2019. NIED K-NET, KiK-net, National Research Institute for Earth Science and Disaster Resilience. https://doi.org/10.17598/NIED.0004.
Sapporo, 2018. Earthquake disaster prevention map - Liquefaction hazard map -. (in Japanese). https://www.city.sapporo.jp/kankyo/ziban_tinka/tyousa.html.
Sapporo, 2019. Survey of ground subsidence in Sapporo – Observation of ground and water level by observation well -. (in Japanese). https://www.city.sapporo.jp/kankyo/ziban_tinka/tyousa.html.
Sapporo City Transportation Bureau Planning Department, 1989. The Sapporo City High Speed Toho Subway Line construction history (between Sakaemachi and Hosui-Susukino). (in Japanese).
Watabe, Y., Nishimura, S., 2020. Ground movements and damages in Satozuka District, Sapporo, due to 2018 Hokkaido Eastern Iburi Earthquake. Soils Found.
Yoshida K., Yoshimi, M., Suzuki, H., Morino, M., Takizawa, F., Sekiguchi, H., Horikawa, H., 2007. 3D velocity structure model of the Ishikari and Yūfutsu sedimentary basins. In: Annual Report on Active Fault and Paleoearthquake Researches, vol. 7, pp. 1–29. (in Japanese).